sustainability

MDPI

Article

Pt(dithiolene)-Based Colorimetric Chemosensors for Multiple Metal-Ion Sensing

Heawon Son [1,†], Seohyeon Jang [2,3,†], Gayoung Lim [1], Taeyong Kim [4,‡], Inho Nam [2,3,*] and Dong-Youn Noh [1,*]

1 Department of Chemistry, Seoul Women's University, Seoul 01797, Korea; shw6094@naver.com (H.S.); addzero@kakao.com (G.L.)
2 Department of Intelligent Energy and Industry, School of Chemical Engineering and Materials Science, Chung-Ang University, Seoul 06974, Korea; tjgus6142@cau.ac.kr
3 Department of Advanced Materials Engineering, Institute of Energy Converting Soft Materials, Chung-Ang University, Seoul 06974, Korea
4 Department of Chemical and Biomolecular Engineering, University of California, Berkeley, CA 94720, USA; kanasis01@gmail.com
* Correspondence: inhonam@cau.ac.kr (I.N.); dynoh@swu.ac.kr (D.-Y.N.)
† These authors contributed equally to this paper.
‡ Present address: Department of Chemical Engineering, Pohang University of Science and Technology (POSTECH), Pohang 37673, Korea.

Abstract: Colorimetric chemosensors are widely employed for in-field analysis to detect transition metal ions in real-time with the naked eye. Colorimetric chemosensors have attracted considerable attention because they can conveniently provide quantitative and qualitative information at a low cost. However, the development of colorimetric chemosensors for multiple-ion sensing where metal cations coexist has been limited. For this reason, we developed a new type of transition metal ion sensing material by selectively replacing functional groups on (diphosphine)Pt(dmit) molecules. The terminal groups of the diphosphine ligand were successfully substituted by the cyclohexyl groups, increasing the electron density of the thione moiety. Due to the electron donation ability of the cyclohexyl terminal groups, the proposed chemosensing material was able to selectively detect the mixture of Hg^{2+}, Cu^{2+}, and Ag^{+} in the presence of many types of interfering cations. To gain insight into the binding mechanisms between the metal ions and the developed (dchpe)Pt(dmit) molecule, density functional theory calculations were also performed.

Keywords: multiple ion detection; colorimetric chemosensors; Pt^{2+}-dithiolene; (dchpe)Pt(dmit); Hg^{2+} ion detection; Cu^{2+} ion detection; Ag^{+} ion detection

Citation: Son, H.; Jang, S.; Lim, G.; Kim, T.; Nam, I.; Noh, D.-Y. Pt(dithiolene)-Based Colorimetric Chemosensors for Multiple Metal-Ion Sensing. *Sustainability* **2021**, *13*, 8160. https://doi.org/10.3390/su13158160

Academic Editors: Hugo Cruz, Gonzalo Guirado, Karolina Zalewska Patricio and Luis Cobra Branco

Received: 29 May 2021
Accepted: 15 July 2021
Published: 21 July 2021

1. Introduction

Repeated exposure to heavy metal ions, such as mercury, lead, copper, and silver from the environment can cause harm to human beings and the ecosystem [1,2]. This issue is complicated by the fact that these elements also have a wide range of important uses in industrial applications. For example, mercury is used in thermometers and sphygmomanometers, while copper and silver are used in the electrical and pharmaceutical industries, as well as in renewable energy. To protect ecosystems from potential toxicity from heavy metal ions and to utilize them for industrial use, it is essential to develop an accurate and cost-effective sensing material.

Colorimetric chemosensors are widely employed for the real-time detection of transition metal ions with the naked eye in field samples. Many studies have reported the use of colorimetric and fluorometric sensors to monitor the trace of transition metal ions from environmental samples [3–6]. Because colorimetric chemosensors produce qualitative (i.e., a visible change in color) and quantitative (i.e., via UV-vis spectroscopy) information at a lower cost and with less effort, they have received greater focus than fluorometric sensors. There was a tremendous effort to enhance the selectivity and sensitivity of the

colorimetric chemosensors toward specific single ions and multiple ions with single sensors [7–13]. It is, however, barely investigated to identify the mixture of heavy metal ions, where a wide range of other metal ions coexist in the environment. In our previous work, Pt-dithiolene-based materials with a diphosphine ligand, denoted as (dxpe)Pt(dmit), were examined by substituting the terminal groups with electron-donating groups to selectively detect mercury cations. Of the tested (dxpe)Pt(dmit) molecules, where dxpe was either 1,2-bis(diphenylphosphino)ethane (dppe) or 1,2-bis[bis(pentafluorophenyl)phosphino]ethane (dfppe) and dmit was 1,3-dithiole-2-thione-4,5-dithiolate, the (dfppe)Pt(dmit) molecule was able to selectively detect Hg^{2+}, while the (dppe)Pt(dmit) molecule detected Hg^{2+}, Cu^{2+}, and Ag^{+} [14,15]. Inspired by the (dppe)Pt(dmit) sensor that can detect three types of single ions, the development of colorimetric chemosensors capable of detecting multiple ions was studied. The developed (dchpe)Pt(dmit) material can detect every single Hg^{2+}, Cu^{2+}, and Ag^{+} ions, while it can also distinguish the combination of each ion simultaneously in the situation of various interfering cations coexisting (dchpe: (1,2-bis(dicyclohexylphosphino)ethane). The structural difference between (dppe)Pt(dmit) and (dchpe)Pt(dmit) is the type of functional group. The (dchpe)Pt(dmit) molecule is synthesized by replacing the phenyl groups of the diphosphine ligand by cyclohexyl groups. With the effect of the electron-donating ability of cyclohexyl groups, the electron density of binding sites in (dchpe)Pt(dmit) was increased. Figure 1 presents a schematic diagram of the interaction between (dchpe)Pt(dmit) and metal ions. The (dchpe)Pt(dmit) is a chelate complex composed of a bidentate dmit ligand and a diphosphine ligand substituted with cyclohexyl groups and both bidentate ligands are connected to a central Pt^{2+} ion. The thione moiety (>C=S) in the dmit ligand is an active site that binds to the target metal ions.

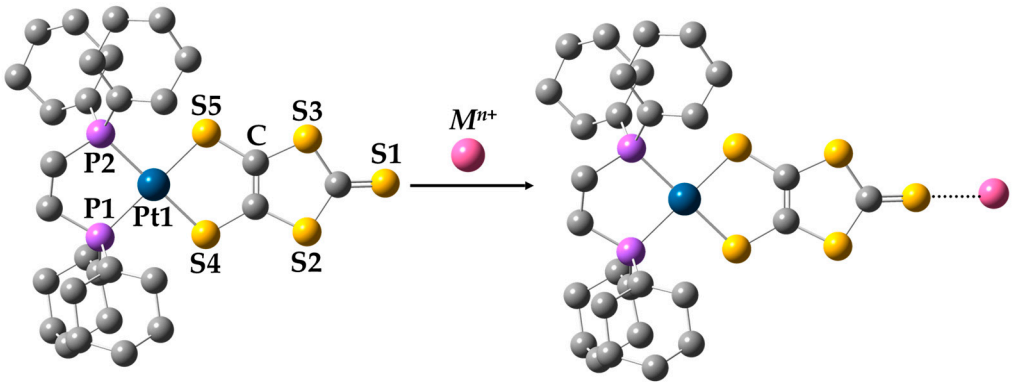

Figure 1. Schematic diagram of the interaction between (dchpe)Pt(dmit) and metal ions (M^{n+}). Hydrogen atoms and solvent molecules are omitted for clarity. Selected bond lengths (Å) and angles (°): Pt1–P2 2.2525(11), Pt1–P1 2.2565(11), Pt1–S5 2.3187(11), Pt1–S4 2.3233(11), P2–Pt1-P1 87.27(4), P2–Pt1-S5 91.20(4), P1–Pt1-S4 91.70(4) and S5–Pt1-S4 90.12(4).

2. Materials and Methods

2.1. Materials

The reagent-grade solvents were dried with a molecular sieve (4 Å) and degassed with N_2 bubbling prior to use. The perchlorate salt of 18 metal ions (M^{n+} = Li^{+}, Na^{+}, K^{+}, Cs^{+}, Mg^{2+}, Ca^{2+}, Ba^{2+}, Al^{3+}, Pb^{2+}, Mn^{2+}, Fe^{2+}, Co^{2+}, Ni^{2+}, Cu^{2+}, Zn^{2+}, Ag^{+}, Cd^{2+} and Hg^{2+}), (COD)$PtCl_2$, dppe, dfppe, and dchpe was purchased from Sigma Aldrich Chemical Company and used without further purification. The dithiolate precursors and *n*-Bu_2Sn(dmit) were prepared according to previously reported methods [16,17]. All reactions and recrystallization processes involving Pt^{2+} were conducted under protection from light and air. The water used in the experiments was distilled 3 times.

2.2. General Characterization

Melting points were determined using a Stuart SMP3 (Barloworld Scientific Ltd., Burlington, NJ, USA). Elemental analysis (C, H, and S) of (dxpe)Pt(dmit) was conducted

using a PerkinElmer 2400 Series II installed at the National Center for Inter-University Research Facilities (NCIRF) at Seoul National University, Seoul, Korea. Measurement of the matrix-assisted laser desorption ionization-time of flight (MALDI-TOF) mass spectra was performed with a Voyager-DETM STR Biospectrometry Workstation (Applied Biosystems Inc., Waltham, MA, USA) installed at NCIRF (Seoul, Korea).

The infrared spectra were recorded on a Nicolet 10 FT-IR spectrometer (Thermo Fischer Scientific Inc., Waltham, MA, USA) within the range of 500–4000 cm^{-1} with an ATR sampling accessory. UV-vis spectra were obtained using a UV-2600 spectrophotometer (Shimadzu Scientific Corp., Kyoto, Japan) using a mixed CH_3CN/CH_2Cl_2 (1:1 v/v%) solution. ^{1}H- and ^{31}P-NMR measurements were taken using an Avance 300 (Bruker, 300 MHz, CD_2Cl_2) and Avance 500 (Bruker, 500 MHz, CD_2Cl_2), respectively, installed at the Korea Basic Science Institute (KBSI), Western Seoul Center, Seoul, Korea.

Electrochemical properties were assessed at room temperature with a computer-controlled potentiostat (ZIVE SP2 Electrochemical Workstation) using a standard three-electrode system with a Pt-disk working electrode, Pt wire as the counter electrode, and saturated Ag/AgCl as the reference electrode. Cyclic voltammograms were obtained in a mixed CH_3CN/CH_2Cl_2 (1:1 v/v%) solution with 1.0 mM samples and a 0.1 M n-$Bu_4N{\cdot}ClO_4$ supporting electrolyte at a scan rate of 100 mVs^{-1}. Ferrocene was used as a calibrant after each set of measurements, and all potentials reported were quoted with reference to the Fc/Fc^{+} redox couple ($E_{1/2}$ = 0.439 V in CH_3CN/CH_2Cl_2 [1:1 v/v%]).

2.3. X-ray Diffraction (XRD) for Molecular Structure Analysis

X-ray structure analysis was performed by a single-crystal diffraction method at the Korea Basic Science Institute (KBSI, Western Seoul Center, Seoul, Korea). A yellow needle-like crystal (0.10 × 0.19 × 0.19 mm^3) of (dchpe)Pt(dmit) was taken up with Paratone oil and mounted on a Bruker SMART CCD diffractometer equipped with a graphite-monochromated Mo Kα (λ = 0.71073 Å) radiation source and a nitrogen cold stream (223 K). Data collection and integration were performed on a SMART (Bruker, Madison, WI, USA, 2000) and SAINT-Plus (Bruker, 2001). Absorption correction was performed by a multi-scan method implemented in SADABS. The structure was solved by direct methods and refined by full-matrix least-squares on F^2 using SHELXTL. All non-hydrogen atoms wererefined anisotropically, and hydrogen atoms were added to their geometrically ideal positions.

2.4. Density Functional Theory (DFT) Calculations

All calculations related to the electronic structure were carried out using the projector-augmented wave (PAW) method for describing ionic cores as implemented in the Vienna Ab initio Simulation Package [18]. First-principles calculations for the geometrical optimization of the chemosensor materials were carried out based on the density functional theory (DFT) using generalized gradient approximation (GGA) within the Perdew-Burke-Ernzerhof (PBE) functional [19,20]. A plane-wave basis set with a kinetic-energy cut-off of 400 eV and 1 × 1 × 1 Monkhorst-Pack k-point mesh was used. The electronic optimization steps were converged self-consistently over 10^{-5} eV per formula unit. The cations adsorbed on each (dchpe)Pt(dmit) molecule in the most stable state were directly relaxed using energy optimization from the initial position. The increase and decrease of electron density around the molecules are marked in gray and purple. In this research, the unit for the charge density was e ${a_0}^{-3}$, where e is the elementary charge and a_0 is the Bohr radius.

2.5. Synthesis

(dchpe)PtCl$_2$ A dichloromethane solution (5 mL) of (COD)$PtCl_2$ (0.40 mmol, 150 mg) was added to a dichloromethane solution (4 mL) of the dchpe ligand (0.45 mmol, 190 mg) under stirring for 4 h at room temperature [21]. The solution was evaporated and recrystallized from hot hexane/$CHCl_3$ using dry ice.

Yield: 71.4% (196.3 mg); MP: >250 °C (decomp.). FT-IR (KBr. cm^{-1}): 2925, 2852 (C-H str), 1445 (-CH_2-), 853, 823, 792, 747 (P-C st); ^{1}H NMR (500 MHz, CD_2Cl_2): δ = 2.38–2.18 (m,

8 H), 1.86–1.69 (m, 20 H), 1.56–1.25 (m, 20 H); ^{31}P NMR (500 MHz, CD_2Cl_2): δ = 65.2 ppm ($J_{Pt\text{-}P}$ = 3574 Hz).

(dchpe)Pt(dmit) A dichloromethane solution (3 mL) of (dchpe)$PtCl_2$ (0.05 mmol, 34.5 mg) was added to an acetone solution (3 mL) of *n*-Bu_2Sn(dmit) (0.05 mmol, 21.4 mg) under stirring overnight at room temperature. The solvent of the mixture solution was reduced via evaporation, followed by the addition of dichloromethane to precipitate the red solid in a vacuum. The product was filtered and recrystallized from dichloromethane/hexane using dry ice.

Yield: 63.1% (51.4 mg); MP: >342 °C (decomp.). Anal. Calcd: C, 42.79; H, 5.94; S, 19.70. Found: C, 43.03; H, 6.08; S, 19.82; FT-IR (cm^{-1}) 2924, 2847 (C-H str), 1445 (-CH_2-), 1053 (C=S), 889(S-C-S), 851,737 (P-C st); UV-vis (CH_3CN/CH_2Cl_2, nm, ε ($M^{-1}cm^{-1}$)) 470 (1.12×10^4); ^{1}H NMR (300 MHz, CD_2Cl_2, TMS): δ = 2.30–1.56 (m, 28 H), 1.50–1.09 (m, 20 H); ^{31}P NMR (202 MHz, CD_2Cl_2): δ = 69.5 ppm ($J_{Pt\text{-}P}$ = 2787 Hz).; MALDI-TOF MS: *m*/*z* (%) 814.0572 (100, $[M]^+$).

(dppe)PtCl$_2$ [7] An ethanol/water solution (80 mL, 1:1 *v*/*v*%) of K_2PtCl_4 (3.0 mmol, 1.245 g) was added to a benzene solution (20 mL) of dppe (3.0 mmol, 1.195 g) under stirring for 24 h at room temperature. After the beige-colored product was filtered, it was washed with distilled water and methanol successively and air dried.

Yield: 94.4% (1.880 g); FT-IR (KBr cm^{-1}): 3051 (Ar CH), 2924 (C-H str.), 1626, 1480, 1436 (Ar C=C), 1309, 1187 (Ar C-H ip def), 1100 (P-Ph), 999, 883 (Ar C-H ip def), 746, 707, 694 (Ar C-H oop def).

(dppe)Pt(dmit) [7] A methanol solution (60 mL) of (dppe)$PtCl_2$ (1.0 mmol, 664 mg) was added to a methanol suspension of Na_2(dmit), and refluxed under stirring for 24 h. The rose-red product was isolated by filtration, washed with methanol, and recrystallized from dichloromethane/hexane.

Yield: 76.1% (582.3 mg); Anal. Calcd: C, 44.10; H, 3.06; S, 20.30. Found: C, 44.19; H, 3.10; S, 21.44; FT-IR (KBr cm^{-1}): 3054 (Ar CH), 2927 (C-H str.), 1482, 1457, 1433, 1402 (Ar C=C), 1307, 1261 (Ar C-H ip def), 1103 (P-Ph), 1051 (C=S), 1029, 999 (Ar C-H ip def), 878 (S-C-S), 744, 717, 705, 688 (Ar C-H oop def); UV-Vis (CH_3CN/CH_2Cl_2, nm, ε ($M^{-1}cm^{-1}$)) 463 (1.23×10^4); ^{1}H NMR (300 MHz, CD_2Cl_2, TMS): δ = 7.81–7.68 (8 H, m, Ph), 7.59–7.43 (12 H, m, Ph), 2.62–2.40 (4 H, m, CH_2C-H); ^{31}P NMR (202 MHz, CD_2Cl_2): δ = 46.6 ppm ($J_{Pt\text{-}P}$ = 2853 Hz); MALDI-TOF MS: *m*/*z* (%) 789.8706 (100, $[M]^+$).

(dfppe)PtCl$_2$ [8] A mixture of dichloromethane solution (11 mL) of (COD)$PtCl_2$ (0.5 mmol, 187 mg) and acetone solution (38 mL) of the dfppe ligand (0.5 mmol, 379 mg) was stirred overnight at room temperature. The mixture solution was evaporated, and the solid was treated with MeOH. The white product was isolated by filtration and recrystallized from dichloromethane/methanol.

Yield: 70.5% (361.0 mg); FT-IR (KBr cm^{-1}): 2929 (C-H str.), 1543, 1519, 1473 (Ar C=C), 1391, 1294, 1090 (P-Ph), 976 (Ar C-F str.).

(dfppe)Pt(dmit) [8] A dichloromethane suspension (30 mL) of (dfppe)$PtCl_2$ (0.5 mmol, 513 mg) was added to an acetone solution (30 mL) of *n*-Bu_2Sn(dmit) (0.5 mmol, 214 mg) under stirring overnight at room temperature in a nitrogen atmosphere. After the mixture solution was evaporated to reduce the volume, a minimum amount of dichloromethane was added to precipitate the red solid in a vacuum. The product was filtered and recrystallized from dichloromethane/methanol.

Yield: 65.0% (373.5 mg); MP: >278 °C (decomp.). Anal. Calcd: C, 30.30; H, 0.35; S, 13.95. Found: C, 31.34; H, 0.35; S, 13.94; FT-IR (KBr cm^{-1}): 1641, 1518, 1473 (Ar C=C), 1392, 1297, 1092 (P-Ph), 1052 (C=S), 976 (Ar C-F st); UV-Vis (CH_3CN/CH_2Cl_2, nm, ε [$M^{-1}cm^{-1}$]) 448 (1.17×10^4); ^{1}H NMR (500 MHz, CD_2Cl_2, TMS): δ = 3.15–3.00 (4 H, m, CH_2C-H); ^{31}P NMR (202 MHz, CD_2Cl_2): δ = 12.7 ppm ($J_{Pt\text{-}P}$ = 2880 Hz); MALDI-TOF MS: *m*/*z* (%) 1149.6199 (100, $[M]^+$).

2.6. Metal-ion Sensing with a Pt^{2+}-Chemosensor

UV-vis measurements were taken to monitor the colorimetric sensing of single metal ions using (dxpe)Pt(dmit) chemosensors. CH_3CN/CH_2Cl_2 solutions (1:1 v/v%) of metal perchlorate (0.4 mM, 1.0 mL) and (dxpe)Pt(dmit) (0.4 mM, 1.0 mL) were mixed to produce a solution of metal ions and the chemosensor with a concentration of 0.2 mM (1:1 v/v%). The absorbance of the mixed solution was measured immediately after mixing the 2 solutions and compared with that of a blank solution containing the chemosensor only.

The multi-metal ion sensing ability of the chemosensors was also examined. CH_3CN/CH_2Cl_2 solutions of metal perchlorates (10 mM each) were mixed in equal amounts and then diluted to a concentration of 0.4 mM. The concentration of each metal ion was maintained at 0.4 mM in all mixed solutions, except for Hg^{2+}, Cu^{2+}, and/or Ag^{+}, which were mixed in different combinations. Mix I was the mixture solution containing all metal ions without Hg^{2+}, Cu^{2+} and Ag^{+}, and Mix II was the mixture solution containing all metal ions without Cu^{2+} and Hg^{2+}. A 1.0 mL solution of (dxpe)Pt(dmit) (0.4 mM) was added to 1.0 mL of the mixed-metal solution (0.4 mM), and the UV-vis absorbance was measured.

2.7. Job's Method

Job's method was carried out using a CH_3CN/CH_2Cl_2 (1:1 v/v%) solution of (dxpe)Pt(dmit) and Hg^{2+} (0.2 mM). The (dxpe)Pt(dmit) solution (1.50–0.00 mL) and the Hg^{2+} solution (0.00–1.50 mL) were mixed, and the total volume of the solution was maintained at 3.00 mL by adding 1.50 mL of CH_3CN/CH_2Cl_2 (1:1 v/v%) solvent. A total of 11 mixtures with different mole fractions (χ) of (dxpe)Pt(dmit) were prepared as summarized in Table 1.

Table 1. The composition of the mixed solution (mL) and the mole fraction (χ) used with Job's method [1].

χ [2]	0.0	0.1	0.2	0.3	0.4	0.5	0.6	0.7	0.8	0.9	1.0
(dxpe)Pt(dmit)	0.00	0.15	0.30	0.45	0.60	0.75	0.90	1.05	1.20	1.35	1.50
Hg^{2+}	1.50	1.35	1.20	1.05	0.90	0.75	0.60	0.45	0.30	0.15	0.00
Solvent [3]	1.50	1.50	1.50	1.50	1.50	1.50	1.50	1.50	1.50	1.50	1.50

[1] Total volume of the CH_3CN/CH_2Cl_2 (1:1 v/v%) solution is 3.0 mL; [2] Mole fraction of (dxpe)Pt(dmit) = [(dxpe)Pt(dmit)]/([Hg^{2+}] + [(dxpe)Pt(dmit)]); [3] CH_3CN/CH_2Cl_2 (1:1 v/v%).

3. Results

3.1. Chemistry

The (dchpe)Pt(dmit) was synthesized and the structure was identified by analyzing XRD, MALDI-TOF mass spectroscopy, UV-vis, ^{31}P NMR, and cyclic voltammetry plots. The (dchpe)Pt(dmit) was synthesized as a new chemosensor by reacting (dchpe)$PtCl_2$ with the dmit-transferring reagent *n*-Bu_2Sn(dmit), as shown in Scheme 1. The product was recrystallized using a two-solvent system. A mixed hot solution of dichloromethane and hexane (1:1 v/v%) with (dchpe)Pt(dmit) was rapidly cooled using dry ice to obtain single crystals. (dfppe)Pt(dmit) was also synthesized in the same way except for the crystallization at room temperature [8]. This preparation strategy is very convenient for isolating the final product because the side-product (*n*-Bu_2SnCl_2) is easily separated using simple filtration. In contrast, (dppe)Pt(dmit) was prepared by mixing (dppe)$PtCl_2$ with the very reactive Na_2(dmit) [7].

The molecular structure of (dchpe)Pt(dmit) was determined using single-crystal X-ray diffraction, for which the crystal data and structure refinement parameters were as follows: monoclinic system; $P2_1/n$; a = 10.1432(3) Å; b = 18.7077(5) Å; c = 19.2779(5) Å; β = 95.3440(10); Z = 4; R_1 = 0.0342, wR_2 = 0.0857. The molecular structure of (dchpe)Pt(dmit) consisted of a P_2PtS_2 core with a square planar geometry and a torsion angle for ∠P1P2S5S4 of 5.94° (Figure 1). The average bond length of Pt-P (2.2545(11) Å) in this compound is very close to that for (dfppe)Pt(dmit) (2.2522(19) Å) and (dppe)Pt(dmit) (2.255(3) Å). However, that of Pt-S (2.3210(11) Å) in (dchpe)Pt(dmit) was longer than that of (dfppe)Pt(dmit) (2.3080(19) Å) and (dppe)Pt(dmit) (2.312(3) Å) [15,22]. The electronegativity of the func-

tional groups substituted on the diphosphine ligand may affect the Pt-S bond length more than that of Pt-P and influence the sensing properties of (dxpe)Pt(dmit) chemosensors.

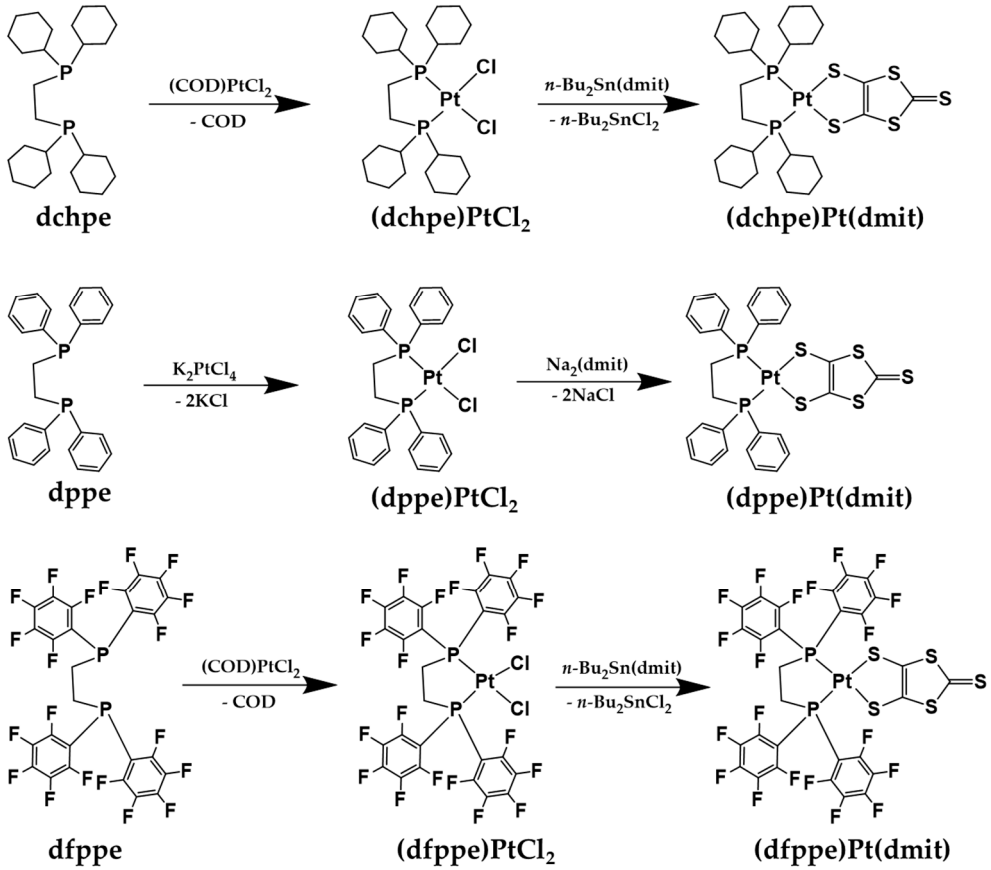

Scheme 1. Synthesis of (dchpe)Pt(dmit) and (dppe)Pt(dmit), and the schematic structures of (dfppe)$PtCl_2$ and (dfppe)Pt(dmit).

To identify the synthesized (dxpe)Pt(dmit) molecules, the MALDI-TOF mass spectra was investigated and compared with the theoretical values in Figure 2. The peaks of analyte ions were observed at 814.0572 m/z for $[(dchpe)Pt(dmit)]^+$, at 789.8706 m/z for $[(dppe)Pt(dmit)]^+$, and at 1149.6199 m/z for $[(dfppe)Pt(dmit)]^+$, with a relative intensity of 100%. The theoretically calculated values were 814.15 m/z for $[(dchpe)Pt(dmit)]^+$, 789.96 m/z for $[(dppe)Pt(dmit)]^+$, and at 1149.76 m/z for $[(dfppe)Pt(dmit)]^+$ and the corresponding mass errors were 107.84 ppm, 113.17 ppm, and 134.90 ppm, respectively. The other peaks indicated the ionized products of (dxpe)Pt(dmit) that can be generated during the measurement process.

UV-vis absorption data for the (dxpe)Pt(dmit) complexes represent the $\pi \rightarrow \pi^*$ transition of the >C=S moiety in the dmit ligand. Those absorption bands exhibited a hypsochromic shift from (dchpe)Pt(dmit) (λmax = 470 nm) to (dfppe)Pt(dmit) (λmax = 448 nm) via (dppe)Pt(dmit) (λmax = 463 nm). That is, the absorption energy for the $\pi \rightarrow \pi^*$ transition in the dmit ligand was positively affected by the diphosphine ligand with the electronegativity of the substituted functional groups [23].This trend was also observed in the ^{31}P NMR spectra of the complexes (Figure 3), with the triplets centered at 69.5 ppm for (dchpe)Pt(dmit), 46.6 ppm for (dppe)Pt(dmit), and 12.7 ppm for (dfppe)Pt(dmit) and with Pt satellites due to Pt-P coupling. The difference in the Pt-P coupling of these compounds is also related to the diphosphine ligand [24]. A diphosphine ligand with a high electron-donating ability undergoes a chemical shift in the low field. Therefore, (dchpe)Pt(dmit), which had the highest electron-donating ability, was de-shielded the most, and (dfppe)Pt(dmit), which had the lowest electron-donating ability, was shielded the

most. This is due to the relationship between the electron density of the central metal and that of the phosphorous lone pair. When the electron-donating ability of the phosphine ligand increases, the electron density of the phosphorous lone pair is removed by donating electrons to the metal orbital, resulting in a downfield shift.

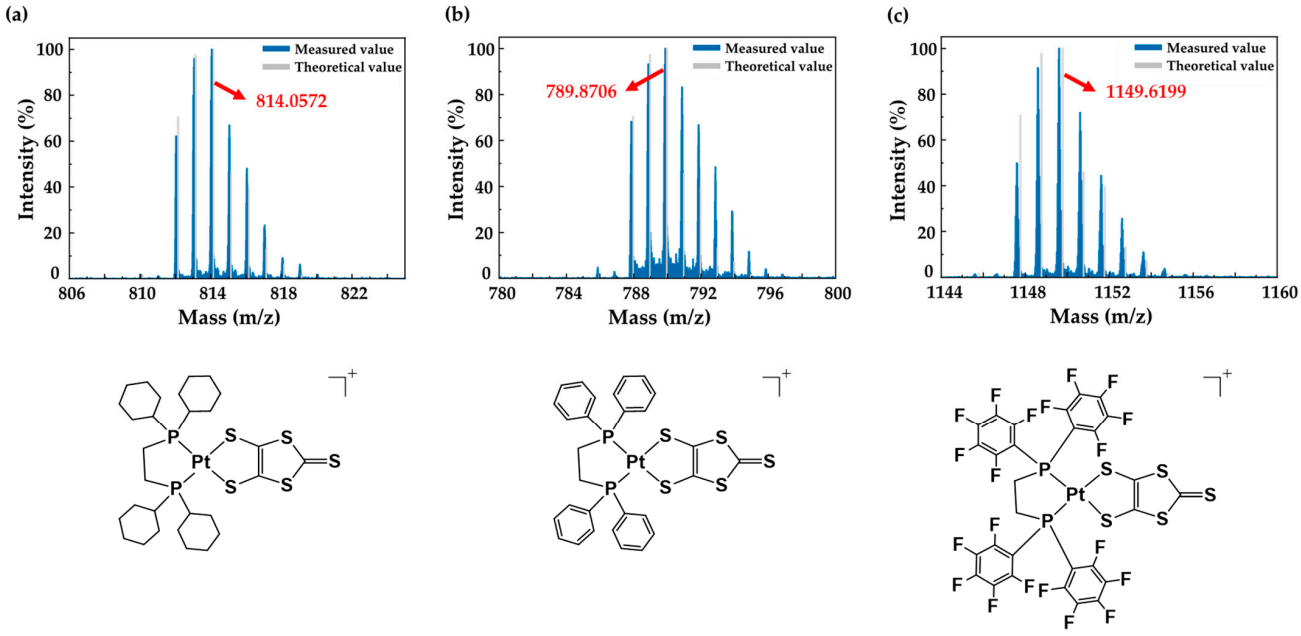

Figure 2. MALDI-TOF mass spectrum of (**a**) (dchpe)Pt(dmit), (**b**) (dppe)Pt(dmit), and (**c**) (dfppe)Pt(dmit). The measured mass-to-charge ratio (m/z) of ionized analyte is indicated in red color with arrow. The structure of ionized analytes are shown below the graph.

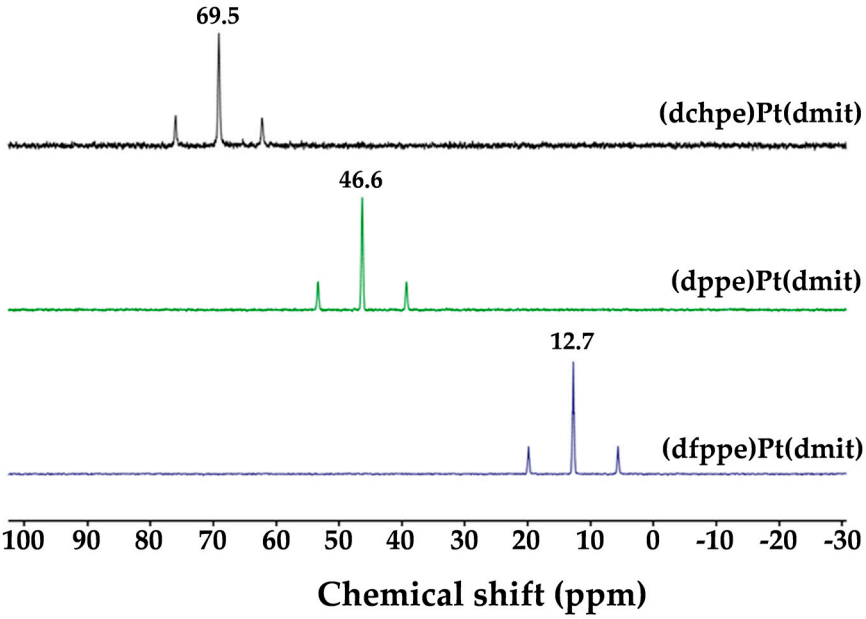

Figure 3. ^{31}P NMR spectra of (dxpe)Pt(dmit) complexes.

Consequently, with the UV-vis and ^{31}P NMR spectroscopic data, it is suggested that the electronegativity of substituted functional groups on the diphosphine ligand affects the electron density of dmit.

The electrochemical properties of (dxpe)Pt(dmit) were investigated with cyclic voltammetry in a CH_3CN/CH_2Cl_2 (1:1 *v*/*v*%) solution (0.1 M *n*-$Bu_4N{\cdot}ClO_4$, Pt-disk working electrode, Ag/AgCl reference electrode). The cyclic voltammograms of (dchpe)Pt(dmit) and (dppe)Pt(dmit) showed one reversible redox cycle at $E_{1/2}$ = 0.681 V (Figure 4a and Table 2) and 0.719 V (Figure 4b), respectively. They were responsible for the $[Pt(dmit)]^{+1/\circ}$ process. However, the corresponding cycle for (dfppe)Pt(dmit) complex was quasi-reversible with $E_{pa}{}^1$ = 0.885 V (Figure 4c), which means that the higher electronegativity of the dfppe ligand was responsible for the higher anodic potential of the $[Pt(dmit)]^{+1/\circ}$ process than that of (dchpe)Pt(dmit) ($E_{pa}{}^1$ = 0.717 V) and (dppe)Pt(dmit) ($E_{pa}{}^1$ = 0.739 V).

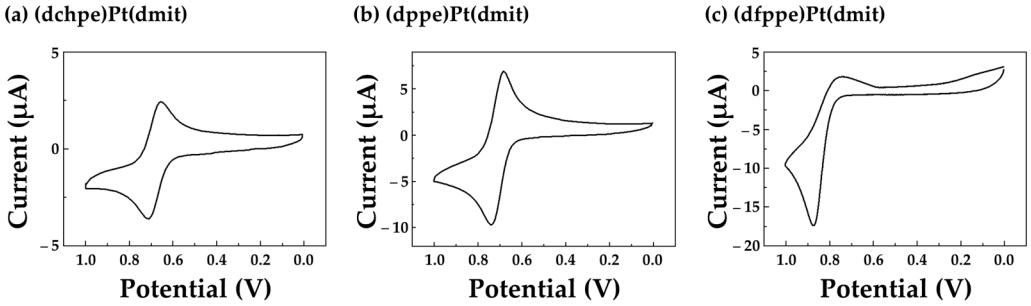

Figure 4. Cyclic voltammograms for (**a**) (dchpe)Pt(dmit), (**b**) (dppe)Pt(dmit), and (**c**) (dfppe)Pt(dmit) measured in CH_3CN/CH_2Cl_2 (Fc/Fc^+ = 0.439 V vs. Ag/AgCl). The insets show reproducible redox cycles scanned three times successively between 0.0 V and 1.0 V.

Table 2. Cyclic voltammetry data for the (dxpe)Pt(dmit) complexes [a].

Complex	$E_{pa}{}^1$	$E_{pa}{}^2$	$E_{pc}{}^1$	$E_{1/2}{}^{1\,b}$
(dchpe)Pt(dmit)	0.717	1.300	0.644	0.681
(dppe)Pt(dmit)	0.739	1.230	0.698	0.719
(dfppe)Pt(dmit)	0.885	1.650	0.736	0.811

[a] 100 mVs^{-1} scan rate, 1.0 mM samples with 0.1 M *n*-$Bu_4N{\cdot}ClO_4$, Pt-disk vs. Pt wire, Ag/AgCl, $E_{1/2}$ = 0.439 V for Fc/Fc^+. [b] $E_{1/2}{}^1 = (E_{pa}{}^1 + E_{pc}{}^1)/2$.

3.2. Colorimetric and UV-Vis Studies

The color change is strongly associated with the electronegativity of the substituted functional groups on the diphosphine ligand. The wider range of metal ions can be detectable by activating the binding site of the (dxpe)Pt(dmit) molecule with substituted EDGs. The binding site of (dxpe)Pt(dmit) molecules is S atom in the thione (>C=S) moiety in the dmit ligand. The dmit ligand is an electron-rich region categorized as a soft base because it bears many π-electrons not only in the >C=S double bond, but also the lone pairs on the S atom. Based on Pearson's acid-base principle, a soft base is likely to interact with soft acids, such as Hg^{2+} rather than hard acids, such as Na^+ and K^+ [25]. Considering the standard reduction potential (E°/V at 298.15 K in water) of the 18 metal ions used in this study, Hg^{2+} (E° = +0.85 V) was expected to interact strongly with the thione moiety on the dmit ligand [24]. It was also expected that Cu^{2+} (E° = +0.34 V) and Ag^+ (E° = +0.80 V) would bind as the number of electrons in the thione moiety became richer (Table 3).

With this basis, preliminary experiments were carried out to analyze the selective reactivity of three types of (dxpe)Pt(dmit) chemical sensors. The perchlorate salts of 18 metal ions were first added to the chemosensor solution under the same conditions, and Figure 5 shows the color changes (M^{n+} = Li^+, Na^+, K^+, Cs^+, Mg^{2+}, Ca^{2+}, Ba^{2+}, Al^{3+}, Pb^{2+}, Mn^{2+}, Fe^{2+}, Co^{2+}, Ni^{2+}, Cu^{2+}, Zn^{2+}, Ag^+, Cd^{2+} and Hg^{2+}). When the metal ions interacted with the chemosensors, the color of the mixed solution changed immediately. The (dchpe)Pt(dmit) and (dppe)Pt(dmit) chemosensors detected Cu^{2+}, Ag^+, and Hg^{2+} because the electron density of the >C=S moiety is enriched by the EDGs (i.e., cyclohexyl groups in (dchpe)Pt(dmit) and phenyl groups in (dppe)Pt(dmit)). The solution changed

from yellow to deep navy when (dchpe)Pt(dmit) and (dppe)Pt(dmit) interact with Hg^{2+}. Furthermore, a slight color change could also be observed with the naked eye when they interacted with Cu^{2+} and Ag^{+}. On the other hand, the (dfppe)Pt(dmit) ligand showed selective reactivity only toward the Hg^{2+} ion with a color change from yellow to purple. The sensing strength of (dfppe)Pt(dmit) is decreased because of the pentaflurophenyl groups, which are strong electron withdrawing groups (EWGs). Because of the lack of electrons on the >C=S moiety, the interaction between (dfppe)Pt(dmit) and the metal ions became relatively weak.

Table 3. Standard Reduction Potentials of the selected metal ions.

Half−Reaction	E° (V)
$Hg^{2+}_{(aq)} + 2\,e^{-} \rightarrow Hg_{(l)}$	+0.85
$Ag^{+}_{(aq)} + e^{-} \rightarrow Ag_{(s)}$	+0.80
$Cu^{2+}_{(aq)} + 2\,e^{-} \rightarrow Cu_{(s)}$	+0.34
$2\,H^{+}_{(aq)} + 2\,e^{-} \rightarrow H_{2\,(g)}$	0.00
$Pb^{2+}_{(aq)} + 2\,e^{-} \rightarrow Pb_{(s)}$	−0.13
$Ni^{2+}_{(aq)} + 2\,e^{-} \rightarrow Ni_{(s)}$	−0.25
$Co^{2+}_{(aq)} + 2\,e^{-} \rightarrow Co_{(s)}$	−0.28
$Cd^{2+}_{(aq)} + 2\,e^{-} \rightarrow Cd_{(s)}$	−0.40
$Fe^{2+}_{(aq)} + 2\,e^{-} \rightarrow Fe_{(s)}$	−0.44
$Zn^{2+}_{(aq)} + 2\,e^{-} \rightarrow Zn_{(s)}$	−0.76
$Mn^{2+}_{(aq)} + 2\,e^{-} \rightarrow Mn_{(s)}$	−1.18
$Al^{3+}_{(aq)} + 3\,e^{-} \rightarrow Al_{(s)}$	−1.66
$Mg^{2+}_{(aq)} + 2\,e^{-} \rightarrow Mg_{(s)}$	−2.37
$Na^{+}_{(aq)} + e^{-} \rightarrow Na_{(s)}$	−2.71
$Ca^{2+}_{(aq)} + 2\,e^{-} \rightarrow Ca_{(s)}$	−2.87
$Ba^{2+}_{(aq)} + 2\,e^{-} \rightarrow Ba_{(s)}$	−2.90
$K^{+}_{(aq)} + e^{-} \rightarrow K_{(s)}$	−2.93
$Cs^{+}_{(aq)} + e^{-} \rightarrow Cs_{(s)}$	−3.03
$Li^{+}_{(aq)} + e^{-} \rightarrow Li_{(s)}$	−3.04

All species are aqueous unless otherwise indicated, and the standard electrode potential is defined as the potential (volts, V) of the half reaction to the reference electrode at 298.15 K in water.

UV-vis measurements were taken to monitor the colorimetric sensing of single metal ions using (dchpe)Pt(dmit) chemosensors. The interaction characteristics of (dchpe)Pt(dmit) and (dppe)Pt(dmit) were analogous, but their absolute values vary significantly. (The UV-vis absorbance spectra of (dppe)Pt(dmit) and (dfppe)Pt(dmit) were examined in our previous work [15]). Figure 6a shows the changes of the absorbance peak of the $\pi \rightarrow \pi^{*}$ transition when (dchpe)Pt(dmit) interacts with single metal ions and the corresponding absorbance ratio (Figure 6b). The UV-vis absorbance spectra show the interaction between the (dchpe)Pt(dmit) and the metal ions. A bathochromic shift is shown from 470 nm to 578 nm (Hg^{2+}), 506 nm with a broad band at 700–800 nm (Cu^{2+}), and 472 nm (Ag^{+}) while the other peaks of metal ions are unchanged.

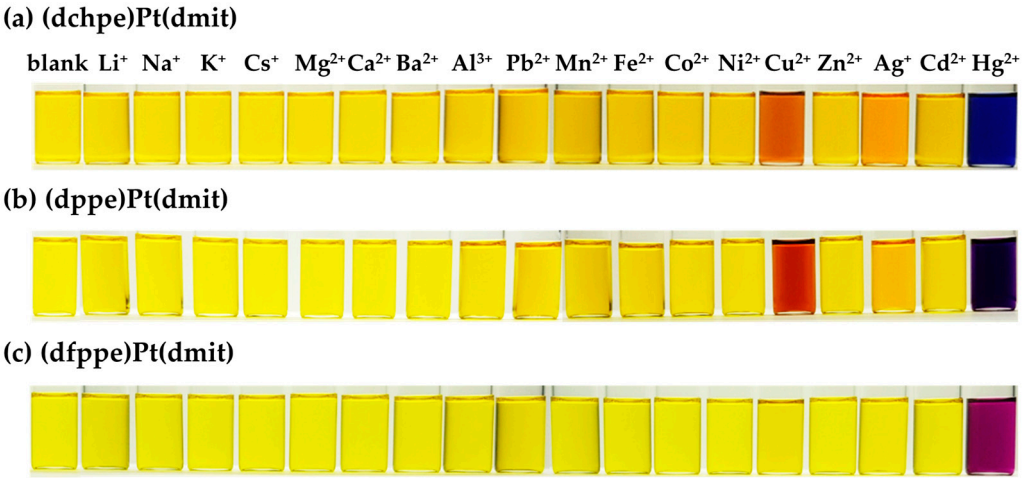

Figure 5. Color changes of the CH_3CN/CH_2Cl_2 solution (0.4 mM, 1:1 v/v%) with (**a**) (dchpe)Pt(dmit), (**b**) (dppe)Pt(dmit), and (**c**) (dfppe)Pt(dmit) following the addition of 1.0 *eq* (0.4 mM) of metal perchlorate salt. Only the (dxpe)Pt(dmit) chemosensors were dissolved in the blank vials.

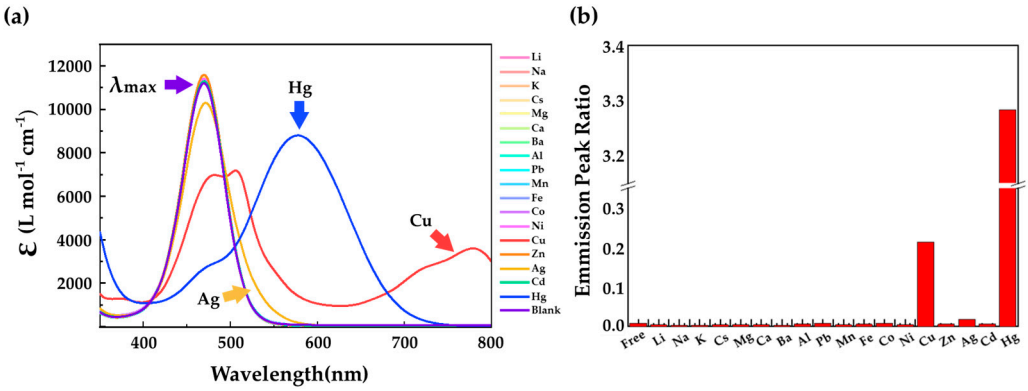

Figure 6. (**a**) Change in the UV-vis spectra in a CH_3CN/CH_2Cl_2 solution (0.2 mM, 1:1 v/v%) containing (dchpe)Pt(dmit) when 1.0 *eq* (0.4 mM) of metal perchlorate is added. (**b**) Absorbance ratios obtained from the UV-vis spectra for (dchpe)Pt(dmit) with or without metal ions dissolved in a CH_2Cl_2/CH_3CN solution (1:1 v/v%).

3.3. Mechanism Study

To determine the ratio of complexation between (dxpe)Pt(dmit) and Hg^{2+}, Job's plots for $Hg(ClO_4)_2$ were drawn. The mole fraction (χ) of (dchpe)Pt(dmit), (dppe)Pt(dmit), and (dfppe)Pt(dmit) was found to be 0.48, 0.50, and 0.51, respectively (Figure 7). This means that (dxpe)Pt(dmit) formed a 1:1 complex with Hg^{2+} in solution, irrespective of the electron-withdrawing ability of the diphosphine ligand.

To gain insight into the binding mechanisms between the metal ions and the (dchpe)Pt (dmit) molecule, DFT calculations were performed. The sulfur atom in the dmit moiety was identified as a binding site, which is capable of forming a chelate complex. The (dchpe)Pt(dmit) molecule acts as a monodentate ligand by donating non-bonding electrons from the sulfur atom to the metal ions. Based on the experimental results, (dchpe)Pt(dmit) exhibited the strongest interaction with Hg^{2+}, followed by Cu^{2+} and then Ag^{+}. To verify the differential selectivity of (dchpe)Pt(dmit) for Hg^{2+}, Cu^{2+}, Ag^{+} and Na^{+} ions on an atomic scale, we calculated the adhesion energy between the active site of (dchpe)Pt(dmit) and the metal ions. In Figure 8, hybridized electrons are shaded in purple (charge accumulation) and grey (charge depletion) and the sulfur atom has a high probability of reacting with heavy metal cations via electrostatic attraction.

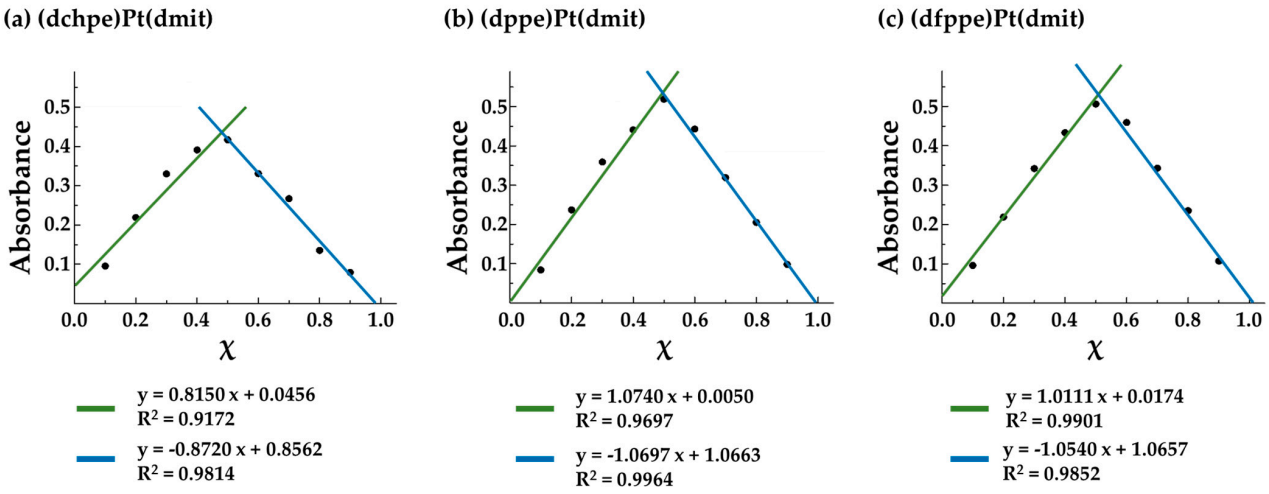

Figure 7. Job's plot for the complexation between (dxpe)Pt(dmit) and Hg^{2+} in CH_3CN/CH_2Cl_2. (**a**) (dchpe)Pt(dmit) with $\chi = 0.48$, (**b**) (dppe)Pt(dmit) with $\chi = 0.50$, and (**c**) (dfppe)Pt(dmit) with $\chi = 0.51$, where $\chi = [Hg^{2+}]/([(dxpe)Pt(dmit)]+[Hg^{2+}])$.

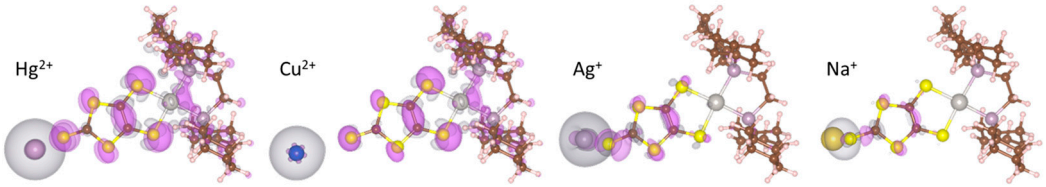

Figure 8. Charge analysis for (dchpe)Pt(dmit) with representative metal ions. The charge accumulation and charge reduction around the molecules are shown in gray and purple, respectively. The isosurface is 0.002e a_0^{-3}, where a_0 is the Bohr radius. Here, the sulfur atom is shown in yellow, Pt in grey, carbon in dark brown, H in pink, and P in purple.

The adhesion energy was examined based on the differential charge density of the sulfur atom using Equation (1). ρ_{total} indicates the charge density of the sulfur atom when the detecting material and metal cations interact, and $\rho_{(dchpe)Pt(dmit)}$ is the charge density of the sulfur atom when single molecules are present without interacting. The results are summarized in Table 4 and the calculated values show a good agreement with the experimental results.

$$\rho_{diff} = \rho_{total} - \rho_{(dchpe)Pt(dmit)} \quad (1)$$

Table 4. Bader atomic charge analyses for the effective charge of the (dchpe)Pt(dmit) complex with and without representative metal ions.

Complex	Δ(−e) [(1)]			
	Hg^{2+}	Cu^{2+}	Ag^{+}	Na^{+}
(dchpe)Pt(dmit)	−1.71	−1.52	−0.61	−0.10

[(1)] Differential effective charge of the metal ions when they coexist with (dchpe)Pt(dmit) molecules.

3.4. Multiple-ion Sensing Ability

The cyclohexyl group is a stronger electron donor than the phenyl group. Both are regarded as EDGs, however, the phenyl group has also electron-withdrawing ability, resulting from the presence of more electronegative sp2 hybridized carbon. For this reason, of the (dxpe)Pt(dmit)-based detection materials that have been proposed, (dchpe)Pt(dmit) showed stronger sensitivity and selectively to distinguish the combination of Hg^{2+}, Cu^{2+}, and Ag^{+} ions than (dppe)Pt(dmit) or (dfppe)Pt(dmit) molecules. To investigate the possibility of multiple-ion sensing, various metal ions were mixed and examined using UV-vis spectroscopy. Here, three types of (dxpe)Pt(dmit) sensing molecule were examined. In this analysis, Mix I and Mix II solutions are prepared, Mix I contains all metal ions except Hg^{2+},

Cu^{2+}, and Ag^{+}, while Mix II contains all metal ions except Hg^{2+} and Cu^{2+}. Mix I was used to examine the multiple-ion sensing behavior of (dchpe)Pt(dmit) and (dppe)Pt(dmit), while Mix II was used to test (dfppe)Pt(dmit). As a first step, a base solution was prepared by adding 1.0 *eq* of Mix I or Mix II to (dxpe)Pt(dmit) solutions. Hg^{2+}, Cu^{2+}, and Ag^{+} ions were then added to the base solution and mixed with various combinations of ions. The color change and absorbance peaks are presented in Figure 9. The absorbance peak of the base solution for (dchpe)Pt(dmit), (dppe)Pt(dmit), and (dfppe)Pt(dmit) was observed at 470 nm, 463 nm, and 449 nm, respectively, with no change in color. The color changes compared to Figures 5 and 9a, illustrated the noticeable effect of interfering metal cations. When (dchpe)Pt(dmit) interacted only with single Hg^{2+}, Cu^{2+}, and Ag^{+} ions, the color changed to navy, deep orange, and deep yellow, respectively (Figure 5); however, in the presence of coexisting cations, the color became ultramarine blue, rose pink, and bright yellow, respectively. The same trend was also observed for (dppe)Pt(dmit) and (dfppe)Pt(dmit). In particular, the (dfppe)Pt(dmit) molecule showed excellent property to distinguish not only single Cu^{2+}, and Hg^{2+} ions, but also multiple ions (Cu^{2+} and Hg^{2+}) (in Figure 9a,d).

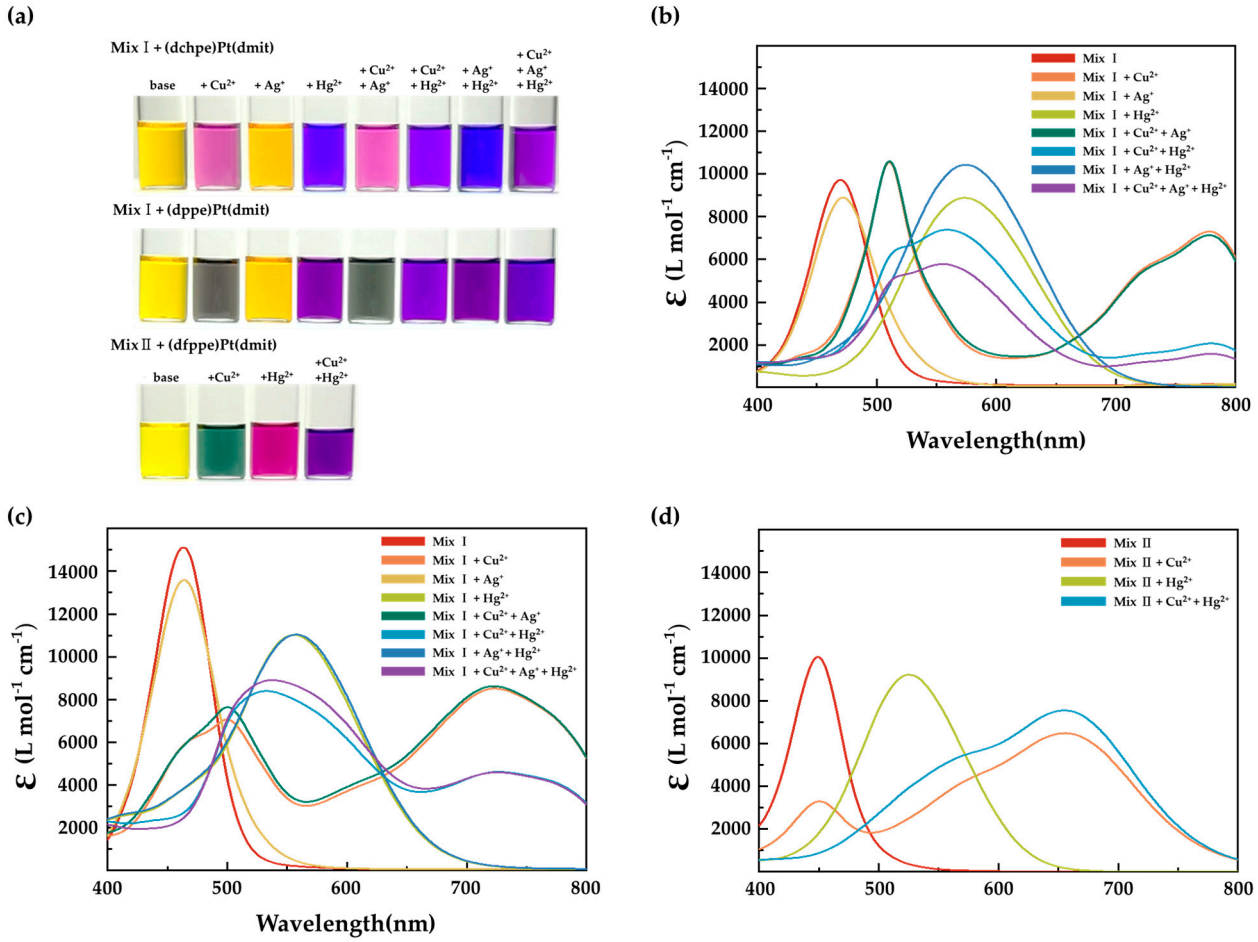

Figure 9. (**a**) Color change for (dxpe)Pt(dmit) after adding metal ions. From left to right; [(dchpe)Pt(dmit) + MixI], + Cu^{2+}, + Ag^{+}, + Hg^{2+}, + Cu^{2+} + Ag^{+}, + Cu^{2+} + Hg^{2+}, + Ag^{+} + Hg^{2+} and + Cu^{2+} + Ag^{+} + Hg^{2+}; [(dppe)Pt(dmit) + MixI], + Cu^{2+}, + Ag^{+}, + Hg^{2+}, + Cu^{2+} + Ag^{+}, + Cu + Hg^{2+}, + Ag^{+} + Hg^{2+} and + Cu^{2+} + Ag^{+} + Hg^{2+}; [(dfppe)Pt(dmit) + MixII], + Cu^{2+}, + Hg^{2+} and + Cu^{2+} + Hg^{2+}. UV-vis spectra for 0.4 mM (**b**) (dchpe)Pt(dmit), (**c**) (dppe)Pt(dmit), and (**d**) (dfppe)Pt(dmit) following the addition of 1.0 *eq* (0.4 mM) of mixed metal perchlorate salts.

This molecule, however, distinguishes only two types of molecule, Cu^{2+} and Hg^{2+}. In contrast, (dchpe)Pt(dmit) and (dppe)Pt(dmit) exhibited potential to detect three types of metal ions, even in the situation where interfering cations coexist. Of the three types of sensing molecule, (dchpe)Pt(dmit) is the most suitable sensing material for practical use as an

analysis tool because it produces more well-distributed color change than (dppe)Pt(dmit), and it can detect three types of metal ions. The color distribution is presented as a CIE 1931 color space chromaticity diagram in Figure 10.

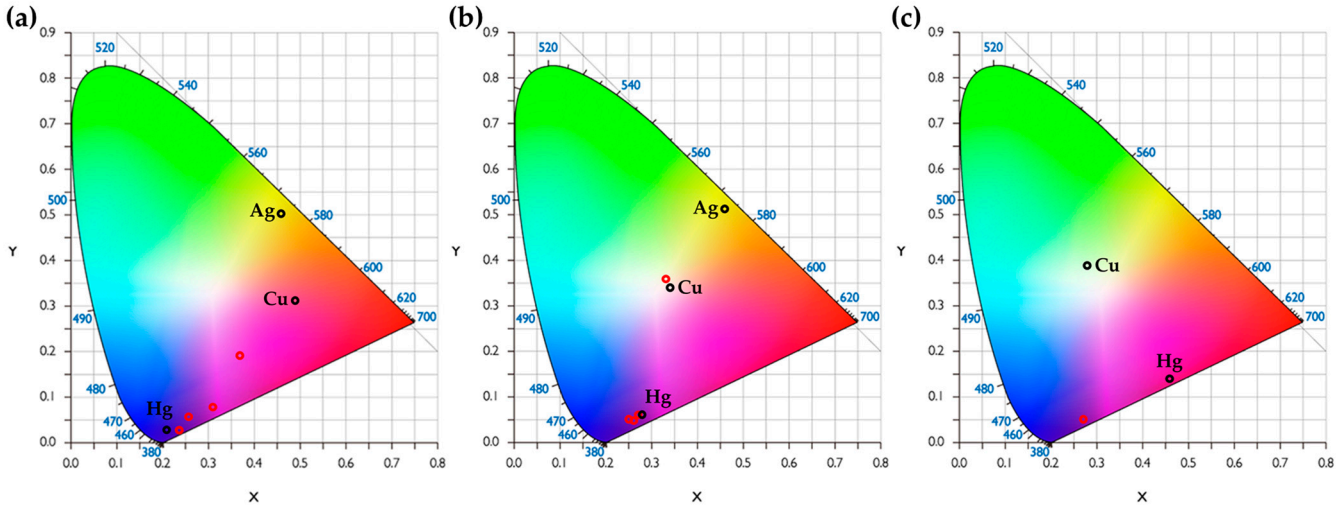

Figure 10. CIE 1931 color space chromaticity diagrams after the interaction between (**a**) the (dchpe)Pt(dmit) ligand and single/multiple ions, (**b**) the (dppe)Pt(dmit) ligand and single/multiple ions, and (**c**) the (dfppe)Pt(dmit) ligand and single/multiple ions. The colors of the multiple ions (Cu^{2+} + Hg^{2+}, Cu^{2+} + Ag^{+}, Hg^{2+} + Ag^{+} and Cu^{2+} + Hg^{2+} + Ag^{+}) are marked by the red circles.

Based on the RGB values in Figure 10a, the colors were expressed as a CIE 1931 color space chromaticity diagram. The chromaticity diagram can be used to determine how the human eye will perceive light with a given spectrum [26]. Color can be divided into brightness and chromaticity. For instance, white is a bright color, while grey is considered to be a less-bright version of that same white. In other words, the chromaticity of white and grey are the same while their brightness differs. In the CIE color space, x and y are projective coordinates and the colors of the chromaticity diagram occupy a region of the real projective plane, and an outer curved boundary is a spectral locus, with the wavelengths shown in nanometers. The chromaticity is then specified by the two derived parameters x and y, with two of the three normalized values being a function of all three tristimulus values X, Y, and Z. The parameters were calculated based using Equations (2) and (3).

$$\begin{bmatrix} X \\ Y \\ Z \end{bmatrix} = \frac{1}{b_{21}} \begin{bmatrix} b_{11} & b_{12} & b_{13} \\ b_{21} & b_{22} & b_{23} \\ b_{31} & b_{32} & b_{33} \end{bmatrix} \begin{bmatrix} R \\ G \\ B \end{bmatrix} = \frac{1}{0.17697} \begin{bmatrix} 0.49000 & 0.31000 & 0.20000 \\ 0.17697 & 0.81240 & 0.01063 \\ 0.00000 & 0.01000 & 0.99000 \end{bmatrix} \begin{bmatrix} R \\ G \\ B \end{bmatrix} \quad (2)$$

$$x = \frac{X}{X+Y+Z} \quad y = \frac{Y}{X+Y+Z} \quad (3)$$

The red circles in Figure 10a show that the colors are well distributed, which indicates that (dchpe)Pt(dmit) is an excellent candidate as a detection material by identifying the type of metal ions in a mixed solution. In contrast, the red circles in Figure 10b for (dppe)Pt(dmit) are more closely grouped together. The proposed (dchpe)Pt(dmit) chemosensor thus appears to have high potential for practical use with real-life environmental samples because it can detect three types of single ions and multiple ions simultaneously.

4. Conclusions

In this study, (dchpe)Pt(dmit) material was synthesized with a two-step reaction pathway and subsequent structural confirmation was conducted using XRD, MALDI-TOF, and CV. The Job's plot and DFT have been used to explain the stoichiometric ratio and binding energies. For field use of colorimetric chemosensors, highly selective and sensitive

reactivity for heavy metal ions is required. Considering the concentration limit of Hg^{2+} for drinking water from EPA (Environmental Protection Agency, USA) regulation, the sensitivity of (dchpe)Pt(dmit) is not sufficient to be used in field analysis [27]. Although the sensitivity still remains as a limitation, the point of this paper is to suggest the possibility of ion mixture sensing ability and methodologies to control the selectivity. Here proposed (dchpe)Pt(dmit) showed good selectivity toward three types of single metal ions (i.e., Hg^{2+}, Cu^{2+}, Ag^{+}) and could analyze the combinations of multiple metal ions over interfering ions. By finely tuning the functional groups the selectivity was successfully enhanced. With the effect of the substituted cyclohexyl functional groups, the electron density on the sulfur atom of thione moiety is increased, facilitating the binding with heavy metal ions.

Author Contributions: Conceptualization, D.-Y.N.; validation, H.S.; formal analysis, S.J. and T.K.; investigation, H.S. and G.L.; resources, D.-Y.N.; writing—original draft preparation, S.J.; writing—review and editing, T.K., I.N. and D.-Y.N.; visualization, S.J.; supervision, I.N. and D.-Y.N. All authors have read and agreed to the published version of the manuscript.

Funding: This work was supported by a National Research Foundation of Korea (NRF) grant funded by the Korean Government (MSIT) (NRF-2020R1C1C1005618) and the Chung-Ang University Graduate Research Scholarship in 2020.

Institutional Review Board Statement: Not applicable.

Informed Consent Statement: Not applicable.

Data Availability Statement: Data available from the corresponding author upon request.

Conflicts of Interest: The authors declare no conflict of interest.

References

1. Park, S.; Johnson, M.A. Awareness of Fish Advisories and Mercury Exposure in Women of Childbearing Age. *Nutr. Rev.* **2006**, *64*, 250–256. [CrossRef]
2. Tchounwou, P.B.; Ayensu, W.K.; Ninashvili, N.; Sutton, D. Environmental exposure to mercury and its toxicopathologic implications for public health. *Environ. Toxicol.* **2003**, *18*, 149–175. [CrossRef]
3. Guo, C.; Irudayaraj, J. Fluorescent Ag Clusters via a Protein-Directed Approach as a Hg(II) Ion Sensor. *Anal. Chem.* **2011**, *83*, 2883–2889. [CrossRef]
4. Shunmugam, R.; Gabriel, G.J.; Smith, C.E.; Aamer, K.A.; Tew, G.N. A Highly Selective Colorimetric Aqueous Sensor for Mercury. *Chem. Eur. J.* **2008**, *14*, 3904–3907. [CrossRef]
5. Fanna, D.J.; Lima, L.M.P.; Wei, G.; Li, F.; Reynolds, J.K. A colorimetric chemosensor for quantification of exchangeable Cu^{2+} in soil. *Chemosphere* **2020**, *238*, 124664. [CrossRef]
6. Guo, X.; Qian, X.; Jia, L. A Highly Selective and Sensitive Fluorescent Chemosensor for Hg^{2+} in Neutral Buffer Aqueous Solution. *J. Am. Chem. Soc.* **2004**, *126*, 2272–2273. [CrossRef]
7. Khan, S.A.; Ullah, Q.; Parveen, H.; Mukhtar, S.; Alzahrani, K.A.; Asad, M. Synthesis and photophysical investigation of novel imidazole derivative an efficient multimodal chemosensor for Cu(II) and fluoride ions. *J. Photochem. Photobiol. A Chem.* **2021**, *406*, 113022. [CrossRef]
8. Khan, S.A.; Ullah, Q.; Almalki, A.S.A.; Kumar, S.; Obaid, R.J.; Alsharif, M.A.; Alfaifi, S.Y.; Hashmi, A.A. Synthesis and photophysical investigation of (BTHN) Schiff base as off-on Cd^{2+} fluorescent chemosensor and its live cell imaging. *J. Mol. Liq.* **2021**, *328*, 115407. [CrossRef]
9. Asiri, A.M.; Al-Amari, M.M.; Ullah, Q.; Khan, S.A. Ultrasound-assisted synthesis and photophysical investigation of a heterocyclic alkylated chalcone: A sensitive and selective fluorescent chemosensor for Fe^{3+} in aqueous media. *J. Coord. Chem.* **2020**, *73*, 2987–3002. [CrossRef]
10. Maiti, S.; Barman, G.; Konar Laha, J. Detection of heavy metals (Cu^{+2}, Hg^{+2}) by biosynthesized silver nanoparticles. *Appl. Nanosci.* **2016**, *6*, 529–538. [CrossRef]
11. Maiti, S.; Prins, L.J. Dynamic combinatorial chemistry on a monolayer protected gold nanoparticle. *Chem. Commun.* **2015**, *51*, 5714–5716. [CrossRef]
12. Maiti, S.; Prins, L.J. A modular self-assembled sensing system for heavy metal ions with tunable sensitivity and selectivity. *Tetrahedron* **2017**, *73*, 4950–4954. [CrossRef]
13. Zhang, S.; Wu, X.; Niu, Q.; Guo, Z.; Li, T.; Liu, H. Highly Selective and Sensitive Colorimetric and Fluorescent Chemosensor for Rapid Detection of Ag^{+}, Cu^{2+} and Hg^{2+} Based on a Simple Schiff Base. *J. Fluoresc.* **2017**, *27*, 729–737. [CrossRef] [PubMed]
14. Jeon, H.; Suh, W.; Noh, D.-Y. Hg(II) sensing properties of (diphosphine)Pt(dmit) complexes (dmit: $C3S52^{-}$: 1,3-dithiole-2-thione-4,5-dithiolate). *Inorg. Chem. Commun.* **2012**, *24*, 181–185. [CrossRef]

15. Jeon, H.; Ryu, H.; Nam, I.; Noh, D.-Y. Heteroleptic Pt(II)-dithiolene-based Colorimetric Chemosensors: Selectivity Control for Hg(II) Ion Sensing. *Materials* **2020**, *13*, 1385. [CrossRef] [PubMed]
16. Doidge-Harrison, S.M.S.V.; Irvine, J.T.S.; Khan, A.; Spencer, G.M.; Wardell, J.L.; Aupers, J.H. Diorganotin 1,3-dithiole-2-thione-4,5-dithiolate compounds, R2Sn(dmit): The crystal structure of MePhSn(dmit). *J. Organomet. Chem.* **1996**, *516*, 199–205. [CrossRef]
17. Nomura, M.; Fourmigué, M. Dinuclear Cp* Cobalt Complexes of the 1,2,4,5-Benzenetetrathiolate Bischelating Ligand. *Inorg. Chem.* **2008**, *47*, 1301–1312. [CrossRef]
18. Grimme, S. Semiempirical GGA-type density functional constructed with a long-range dispersion correction. *J. Comput. Chem.* **2006**, *27*, 1787–1799. [CrossRef]
19. Perdew, J.P.; Burke, K.; Ernzerhof, M. Generalized Gradient Approximation Made Simple. *Phys. Rev. Lett.* **1996**, *77*, 3865–3868. [CrossRef]
20. Kresse, G.; Furthmüller, J. Efficient iterative schemes for ab initio total-energy calculations using a plane-wave basis set. *Phys. Rev. B* **1996**, *54*, 11169–11186. [CrossRef]
21. Hackett, M.; Whitesides, G.M. [Bis(dicyclohexylphosphino)ethane]platinum(0). Reactions with alkyl, (trimethylsilyl)methyl, aryl, benzyl, and alkynyl carbon-hydrogen bonds. *J. Am. Chem. Soc.* **1988**, *110*, 1449–1462. [CrossRef]
22. Vicente, R.; Ribas, J.; Solans, X.; Font-Altaba, M.; Mari, A.; de Loth, P.; Cassoux, P. Electrochemical, EPR, and crystal structure studies on mixed-ligand 4,5-dimercapto-l,3-dithia-2-thione phosphine complexes of nickel, palladium and platinum, M(dmit)(dppe) and Pt(dmit)(PPh3)2. *Inorg. Chim. Acta* **1987**, *132*, 229–236. [CrossRef]
23. Shin, K.-S.; Jung, Y.; Lee, S.-K.; Fourmigué, M.; Barrière, F.; Bergamini, J.-F.; Noh, D.-Y. Redox bifunctionality in a Pt(ii) dithiolene complex of a tetrathiafulvalene diphosphine ligand. *Dalton Trans.* **2008**, 5869–5871. [CrossRef]
24. Bratsch, S.G. Standard Electrode Potentials and Temperature Coefficients in Water at 298.15 K. *J. Phys. Chem. Ref. Data* **1989**, *18*. [CrossRef]
25. Pearson, R.G. Hard and Soft Acids and Bases. *J. Am. Chem. Soc.* **1963**, *85*, 3533–3539. [CrossRef]
26. Orava, J.; Jääskeläinen, T.; Parkkinen, J.; Leppanen, V.-P. Diffractive CIE 1931 chromaticity diagram. *Color Res. Appl.* **2007**, *32*, 409–413. [CrossRef]
27. Agency for Toxic Substances and Disease Registry (ATSDR). *Toxicological Profile for Mercury*; U.S. Department of Health and Human Services, Public Health Service: Atlanta, GA, USA, 1999.